JMB

Islet Amyloid Polypeptide: Identification of Long-range Contacts and Local Order on the Fibrillogenesis Pathway

Shae B. Padrick and Andrew D. Miranker *

Department of Molecular Biophysics and Biochemistry Yale University, 266 Whitney Avenue, PO Box 208114, New Haven, CT 06520, USA

The pathology of type II diabetes includes deposition of amyloid in the extra cellular space surrounding the b-cells of the endocrine pancreas. The principle component of these deposits is an insoluble fibrillar form of a normally soluble 37 residue peptide hormone, islet amyloid polypeptide. Multiple sequence analysis and peptide synthesis have identified a core set of residues (20 to 29) as intrinsically amyloidogenic. As the fibrillogenesis of the 20-29 peptide often requires conditions that deviate considerably from physiological, residues 20 to 29 may be necessary, but not sufficient, for amyloidosis. We aim to determine the structural role of residues outside this core in the context of in vitro fibrillogenesis of the wild-type peptide at physiological pH and ionic strength. Specifically, we make use of an intrinsic fluorescent probe, tyrosine 37 (Y37), to explore the role of the C terminus in fibrillogenesis. Our protocol permits steady state measurement of the lag phase and fiber conformational states of the protein under identical conditions. These are compared to a non-amyloidogenic variant of islet amyloid polypeptide from rat and N-acetyl-tyrosinamide as models of the unfolded state under matched conditions. Spectral, quenching and anisotropic properties of Y37 in the fiber state indicate that the C terminus is packed in a well-defined environment with near frozen rigidity. The presence of a fluorescence resonance energy transfer pathway shows Y37 is near F15 and F23. The lag-phase conformation, while considerably less ordered than the fiber, is more ordered than unfolded models. Differences in anisotropy between the lag and fiber state were used to monitor fibrillogenesis in real time. Parallel assessment of fiber formation using the histological dye, ThT, indicate that ordering at the C terminus of islet amyloid polypeptide is coincident with, and thus indicative of, fiber formation.

2001 Academic Press

*Corresponding author

Keywords: IAPP; tyrosine fluorescence; type II diabetes; amyloid; amylin

Introduction

The deposition of normally soluble protein as amyloid fiber is central to a number of diseases including, for example, Alzheimer's and dialysis related amyloidosis.[1] This problem is particularly fascinating as proteins that are apparently unrelated in sequence and in their native conformations nevertheless aggregate into fibrils with common structural and histological features.[2] These features include a crossed-b sheet organization in which the b-strands are arranged perpendicular to the fibril axis, and the display of green birefringence upon binding of the dye Congo Red. Amyloid fiber formation kinetics also share common features.[3] Fibrillogenesis reactions are characterized by a lag phase during which no fibers are observed. This is then followed by a period of fiber formation on a timescale that can be shorter than the lag phase. Furthermore, the lag phase can often be bypassed by nucleating a reaction with preformed fibers.

Abbreviations used: FRET, fluorescence resonance energy transfer; IAPP, islet amyloid polypeptide; hIAPP, human IAPP; hIAPP$_{lag}$, the lag phase conformation of hIAPP; hIAPP$_{fib}$, the fibrillar conformation of hIAPP; rIAPP, rat IAPP; HFIP, 1,1,1,3,3,3-hexafluoroisopropanol; NAYA, N-acetyl tyrosinamide; nMAC, N-methyl acetamide; ThT, Thioflavin T.
E-mail address of the corresponding author: Andrew.Miranker@yale.edu

Greater than 90 % of type II diabetics have amyloid deposits surrounding the islet cells of the pancreas[4] These deposits are predominantly made of fibers composed of islet amyloid polypeptide (IAPP). IAPP is a 37-residue peptide which is co-secreted with insulin by the b cells. A number of possible metabolic roles have been suggested for IAPP, e.g. slowing of pyloric emptying into the duodenum[5] and attenuation of insulin secretion by b cells.[6] Increased insulin secretion (and therefore IAPP secretion) is the normal response to insulin resistance in type II diabetics. As IAPP fibers have been shown to be toxic to cultured b cells,[7] the development of IAPP fibers is thought to amplify the diabetic state through severe depletion in the number of b cells available to secrete insulin.

The covalent structure of IAPP in diabetics is identical to that found in healthy individuals. Furthermore, in vitro fiber formation occurs at IAPP concentrations below the concentration found in the secretory granule (ca 400 mM).[8-10] This implies that a change in the environment of IAPP is responsible for the conformational change to insoluble amyloid fiber in diabetics. Subsets of the IAPP sequence, e.g. 20-29[11] and 30-37[12] have been characterized and shown to form fibers. Independent fiber formation by these peptides suggests that they may be in a similar conformation to that seen for the same stretch of amino acid residues in the full-length fiber. We note, however, that the concentrations required for fiber formation by these sequences are often orders of magnitude higher than that required for the full-length peptide. This suggests that additional interactions are necessary for the formation and stability of wild-type IAPP fibers.

Here, we have used the intrinsic aromatic residues of IAPP to study conformational change induced by fibrillogenesis of the full-length peptide. As wild-type IAPP possesses a single tyrosine and no tryptophans (Figure 1), we are able to make several specific and complementary studies of this residue. Excitation and emission profiles, steady state anisotropy, quenching behavior and resonant energy transfer between internal aromatics are all used to develop a structural description of IAPP prior to and after fibrillogenesis.

Results

Polymerization time for human IAPP (hIAPP) is strongly dependent on reaction conditions and procedures for preparation of stock solutions.[13] For this work, we chose a single reaction condition that

reproducibly generates a lag phase in excess of ten minutes with fibrillogenesis complete in less than 1 hr (Figure 2). We refer to the conformational ensemble of hIAPP before fibrillogenesis as hIAPP$_{lag}$ and after fibrillogenesis as hIAPP$_{fib}$. Our time-scale is determined from the midpoint, $t_{1/2}$, for maximal fluorescence enhancement of the histological dye, Thioflavin T (ThT)[14] (Figure 2). The reaction (initiated by a 1:40 dilution of a 1 mM stock solution of hIAPP in HFIP, with 100 mM KCl, 50 mM potassium phosphate (pH 7.4) at 25 °C) yields a final protein concentration of 25 mM. This readily permits steady state intrinsic fluorescence measurements to be conducted before and after the transition. There are three fluorescent residues in hIAPP: F15, F23 and Y37 (Figure 1). The maximum absorbance of tyrosine is $e_{275} \approx 1.4 \, f f i 10^3 \, M^{-1} \, cm^{-1}$ while that of phenylalanine is $e_{255} \approx 0.22 \, f f i 10^3 \, M^{-1} \, cm^{-1}$.[15] Furthermore, the quantum yield of fluorescence for tyrosine is approximately fourfold higher than for phenylalanine. We can assume, therefore, that light detected upon excitation at 278 nm is entirely derived from Y37.

Two reference molecules are used to evaluate hIAPP$_{lag}$ and hIAPP$_{fib}$ under matched solution conditions. As a baseline for interpretation of fluorescence, we use a tyrosine analogue. Our choice, N-acetyl-tyrosinamide (NAYA), reflects the presence of C-terminal amidation in IAPP. As a model of the unfolded state, we use a sequence variant of IAPP from rat (rIAPP) (Figure 1). The relevance of rIAPP to these studies is derived from two observations. First, the far UV CD spectrum of rIAPP under our reaction conditions is characteristic of a random coil (data not shown).[13] Second, although rIAPP is 84 % identical to hIAPP, it is non-amyloidogenic. This has been attributed to the presence of three proline residues, which are known to be strong b-sheet breakers.[16] These two reference molecules permit changes in the spectral properties of rIAPP versus hIAPP$_{lag}$ and hIAPP$_{lag}$ versus hIAPP$_{fib}$ to be interpreted in terms of unfolded to lag-phase and lag-phase to fiber structural transitions, respectively.

Electronic environment of Y37

The excitation maximum for NAYA under our reaction conditions is 275 nm (Figure 3(a)), excitation of which yields an emission profile with a maximum at 300 nm (Figure 3(b)). At wavelengths that are longer than their peak maxima, the excitation profile of NAYA, rIAPP, hIAPP$_{lag}$ are nearly

```
hIAPP    KCNTATCATQRLAN F LV H SSNN F GAI L SS TNVGSNT Y -NH2
rIAPP    KCNTATCATQRLAN F LV R SSNN L GPV L PP TNVGSNT Y -NH2
 NAYA                                              Ac- Y -NH2
        ........10........20........30.......
```
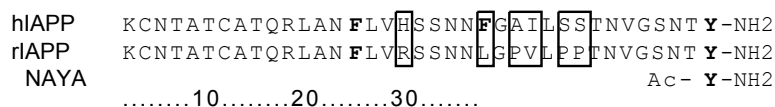
Figure 1. Amino acid sequence of hIAPP, rIAPP, and NAYA. NAYA is shown here schematically. Changes between hIAPP and rIAPP sequences are in boxes. Intrinsic fluorescent aromatic residues are highlighted in bold.
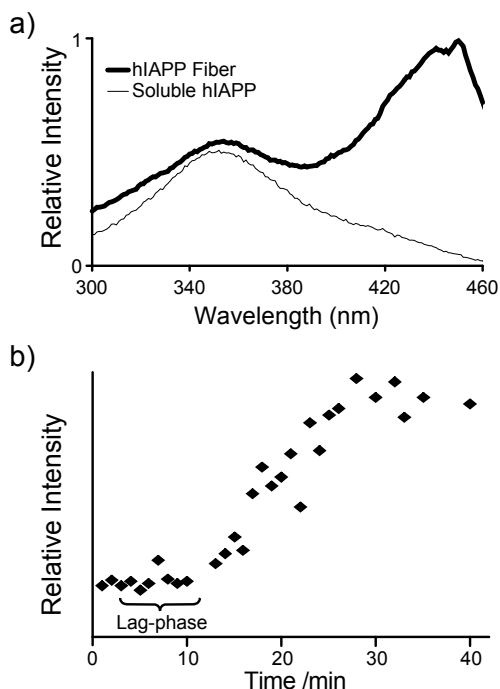
a)

b)

Figure 2. Fiber formation kinetics followed by ThT fluorescence. (a) Fluorescence of ThT is enhanced upon binding fiber. hIAPP as preformed fibers (thick line), or monomer stock solution in HFIP (thin line) was diluted to identical concentration (in monomer units) with ThT containing buffer. For fibers, the fluorescence excitation spectrum between 430 and 460 nm is dramatically increased. Emission is detected at 482 nm. (b) Kinetics followed by ThT fluorescence. Aliquots of a standard fiber formation reaction are removed at successive time points and quenched by dilution with ThT assay buffer. Excitation intensities are integrated from 430-460 nm.

identical (Figure 3(a)). By contrast, the relative intensity of excitation transitions at these longer wavelengths is greater for $hIAPP_{fib}$. An increase in relative intensity at wavelengths near 287 nm has also been observed in absorbance and fluorescence excitation measurements of the interaction of free tyrosine with peptide backbone mimics, such as N-methyl acetamide (nMAC).[17,18] These investigations have suggested that these lower energy transitions are enhanced when the tyrosine hydroxyl oxygen accepts a hydrogen bond. We made an analogous study under our reaction conditions by determining the difference spectrum of NAYA in the presence and absence of 1 M nMAC (Figure 3(c)). Comparing this to the difference spectrum of NAYA and $hIAPP_{fib}$ clearly shows similarities at wavelengths above 275 nm.

Excitation profiles at wavelengths that are shorter than 265 nm show a clear progression in the fluorescent intensity of rIAPP, $hIAPP_{lag}$ and $hIAPP_{fib}$ compared to NAYA (Figure 3(a)). This is most

readily seen at 250 nm. As this is 24.5 nm below the excitation maximum for NAYA and as the slope of the excitation of NAYA at 250 nm can be seen approaching 0, it seems unlikely that intensity at this wavelength is the result of direct excitation of tyrosine. One possibility is that this trend is the result of excitation of phenylalanine. As we collect emission 25 nm above the emission I_{max} phenylalanine and, since the quantum yield for phenylalanine is 1/4 that of tyrosine, our observations would reflect fluorescence resonance energy transfer (FRET), not direct emission of phenylalanine. This can occur with measurable efficiency, for example in histone-like protein from Thermoplasma acidophilum,[19] provided the distance between donor (F) and acceptor (Y) is less than 18 Å (efficiency ˆ 10 %).

To confirm that our observation is due to FRET, we first compared the difference spectrum of $hIAPP_{fib}$ and NAYA with the excitation spectrum of free phenylalanine (Figure 3(c)). A correspondence can clearly be seen at wavelengths below 270 nm. Second, we were able to monitor the quenching of the phenylalanine fluorescence by the presence of the acceptor, tyrosine (Figure 3(d)). By monitoring emission at 278 nm rather than 303 nm, we ensured that fluorescence of phenylalanine would predominate over that of tyrosine. The excitation spectrum of $hIAPP_{lag}$ clearly shows a maximum at 258 nm indicating that some direct emission of phenylalanine fluorescence can still be measured from this conformational state. Upon fiber formation, a distinct peak for phenylalanine fluorescence is no longer observed. This indicates complete quenching of the fluorescence of both phenylalanine residues.

Emission profiles of rIAPP and $hIAPP_{lag}$ are indistinguishable from NAYA (Figure 3(b)), although intensities are diminished by ☐80 % (Figure 3(b), inset). This loss of intensity between free tyrosine and tyrosine incorporated in peptides is well known and largely attributed to quenching by the carbonyl group of peptide bonds.[17,20] By contrast, the emission profile of $hIAPP_{fib}$ differs markedly from NAYA. A substantially greater proportion of $hIAPP_{fib}$ emission is at wavelengths that are shorter than the maximum (300 nm). While this is due in part to a small increase in the direct scatter intensity brought about by the presence of fibers, scatter cannot account for the diminishment of intensity above 300 nm. Blue shifts in tryptophan fluorescence are commonly attributed to burial of the indole moiety in the hydrophobic core of a protein. This does not follow for tyrosine as its emission is far less sensitive to environment. Emission I_{max} of phenol derivatives such as NAYA, for example, is unchanged in solvents as diverse as water and 1,4-dioxane.[17]

Solvent accessibility of the C terminus

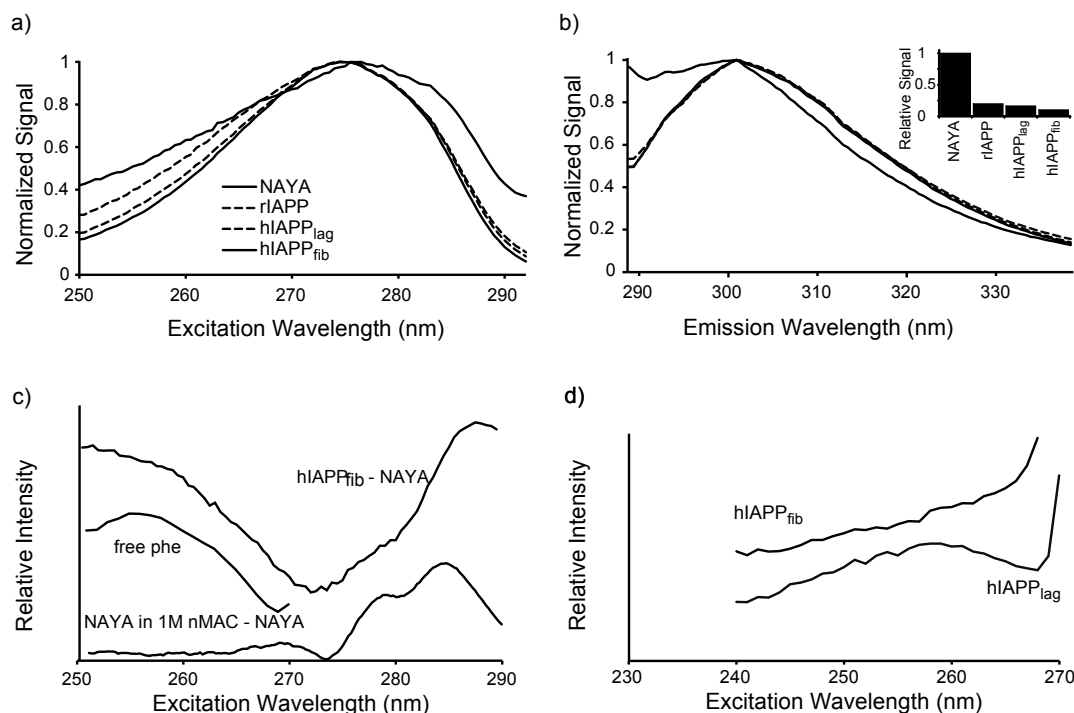The excited state of tyrosine, as any fluorophore, returns to the ground state via a number of path-

Figure 3. Intrinsic fluorescence of IAPP. (a) Normalized fluorescence excitation spectra for NAYA, rIAPP, hIAPP$_{lag}$ and hIAPP$_{fib}$. All spectra acquired under identical conditions. Emission is observed at 303 nm. (b) Normalized fluorescence emission spectra for NAYA, rIAPP, hIAPP$_{lag}$ and hIAPP$_{fib}$. All spectra acquired under identical conditions. Excitation wavelength is 278 nm. Curve identities are shown in (a). The spectra for NAYA, rIAPP and hIAPP$_{lag}$ overlay. (Inset) Relative fluorescent intensity for samples in (a) and (b). Intensities measured at excitation wavelength 275 nm and emission wavelength 300 nm. IAPP concentrations were 25 mM in all samples. NAYA concentration 5 mM and scaled by 5. (c) Difference spectrum of hIAPP$_{fib}$ and NAYA shown in (a). Two distinct peaks are observed, one with a l$_{max}$ above 278 nm, the other below. An excitation spectrum of 500 mM free phenylalanine is shown (emission observed at 278 nm), and corresponds to the blue shifted peak of hIAPP$_{fib}$-NAYA. The difference spectrum of [NAYA in 1 M nMAC]-[NAYA in H$_2$O] and corresponds to the red shifted peak of hIAPP$_{fib}$-NAYA. Curves have been offset for clarity. Latter curve was smoothed using a 2 nm rolling average. (d) Fluorescence excitation spectrum of hIAPP, detecting at 278 nm. A peak for phenylalanine is readily apparent in hIAPP$_{lag}$ and absent in hIAPP$_{fib}$.

ways, of which, only one is emission of a photon detectable as fluorescence. The proportion of molecules that emit a photon can be greatly diminished by addition of a soluble quenching agent to the solution. Quenching is dependent, in part, on contact of the quenching agent with the fluorophore. This provides an effective means of characterizing the local environment of a fluorophore in terms of solvent accessibility, e.g. Garzon-Rodriguez et al.[21] We have made use of this to study the conformation of IAPP in terms of the solvent accessibility of Y37.

The effect of the quenching agent, acrylamide, was determined for NAYA, rIAPP, hIAPP$_{lag}$ and hIAPP$_{fib}$ over a quenching agent concentration range of 0 to 100 mM (Figure 4(a)). As expected, NAYA is most easily quenched with 60 % of the fluorescence intensity lost at 100 mM acrylamide. By comparison, the extent to which rIAPP is

quenched by 100 mM acrylamide is smaller. The difference between rIAPP and NAYA most likely stems from the slower diffusion of rIAPP. Quenching of Y37 in hIAPP$_{lag}$ shows a further reduction over rIAPP. While the difference is small, it is consistent and is also qualitatively observed when I$^-$ is used as the quenching agent. The difference between rIAPP and hIAPP$_{lag}$ is most readily explained by a conformational difference between the two that either affords a greater degree of solvent protection for Y37 in hIAPP$_{lag}$ or a significantly larger hydrodynamic radius for hIAPP$_{lag}$.

Conversion of hIAPP$_{lag}$ to a fibrillar state results in a dramatic reduction in the sensitivity of Y37 to quenching. At 100 mM acrylamide, fluorescence in hIAPP$_{fib}$ is reduced by only 39 % compared to 51 % in hIAPP$_{lag}$. A reduction in quenching may result from either solvent exclusion, or a reduced diffusion rate. Collisional quenching is, however,
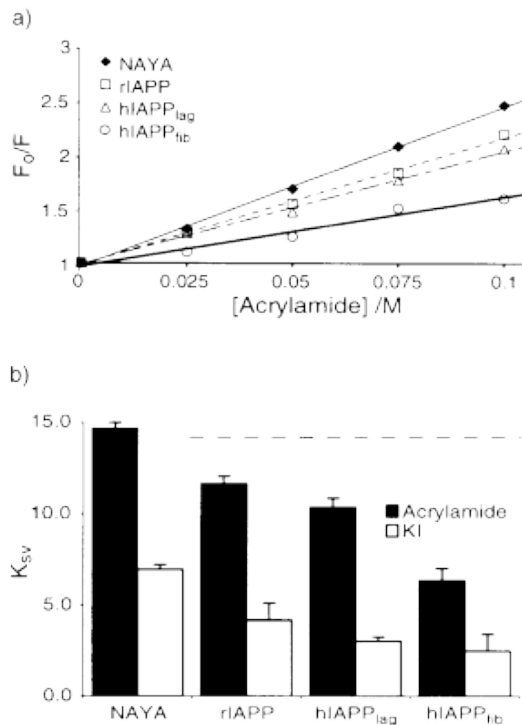
Figure 4. Measurement of solvent accessibility by quenching of intrinsic fluorescence. (a) Stern-Volmer analysis of quenching of IAPP fluorescence by acrylamide. Data was fit to the equation $F_0/F ^ K_{SV}[Q] \ddagger b$, where F is the fluorescence intensity at concentration [Q] of quencher. For clarity, points shown are averages of three measurements, although statistics were determined using all points. All lines extrapolate back to $b ^ 1(\square 0.03)$ at $[Q] ^ 0$ M. Pearson's R for fits of acrylamide quenching are 0.997, 0.994, 0.985, and 0.944 for NAYA, rIAPP, hIAPP$_{lag}$ and hIAPP$_{fib}$, respectively. (b) Values of K_{SV} for quenching of tyrosine fluorescence by acrylamide (filled bars) or iodide (open bars). Heavy line at $K_{SV} ^ 14.2 M^{-1}$ represents a theoretical estimate of acrylamide quenching (see Materials and Methods) for a 100 % solvent exposed tyrosine in monomeric IAPP being quenched by acrylamide. Error bars are the standard error in the slope of the fit.

proportional to the sum of the fluorophore and quencher diffusion rates.[15] As the diffusion rate for both hIAPP$_{lag}$ and hIAPP$_{fib}$ is small in comparison to that of acrylamide, diminished sensitivity of hIAPP$_{fib}$ to quenching reflects burial of Y37.

Quenching can arise from either binding of quenching agent, or diffusion controlled collisions. Furthermore, multiple protein conformations may contribute to the observed quenching behavior. To address these issues, fluorescence in the absence of quenching agent (F_o) and as a function of quenching agent concentration (F) was measured. Plots of F_o/F as a function of acrylamide concentration (Stern-Volmer analysis) show linear behavior.

Furthermore, the fits consistently extrapolate to an intercept of $1(\square 0.03)$ (Figure 4(a)). This strongly suggests that only single conformers are contributing to our observations. The slopes of the fits, K_{SV}, describe the ease of quenching in a physically interpretable way. Our measurements were repeated using I⁻ as the quenching agent (Figure 4(b)). The trends observed for acrylamide and I⁻ are similar, although the absolute magnitudes are not. The reduced degree by which I⁻ quenches compared to acrylamide likely reflects its reduced quenching efficiency. The similarity of the behavior of the two quenching agents suggests that the quenching of Y37 in IAPP is the result of diffusion-controlled collisions of quenching agent with phenol groups that are in structurally homogeneous environments.

An independent approach to measuring solvent accessibility is the measurement of the pK_a of the tyrosine. If buried or partially buried, tyrosine will ionize at an increased pK_a.[22] Tyrosinate, tyrosine's conjugate base, has dramatically less fluorescent intensity at 303 nm. Therefore, we can measure the pK_a of tyrosine by monitoring the loss of fluorescent intensity as a function of pH (Figure 5). We presumed that hIAPP$_{lag}$ would be affected by pH and therefore measured the pK_a of tyrosine in NAYA, rIAPP and hIAPP$_{fib}$ only. Subsequent ThT analysis of hIAPP$_{fib}$ samples incubated at these pH values showed a <10 % variation in fiber content. NAYA exhibits a pK_a of 9.9, which is a commonly observed value for tyrosine pK_a. Titration of rIAPP yields data within error to that of NAYA (data now shown). hIAPP$_{fib}$ however shows a pK_a which is increased by nearly two full pK_a units, to a pK_a of 11.8. We attribute this shift to partial hydrophobic burial of Y37.
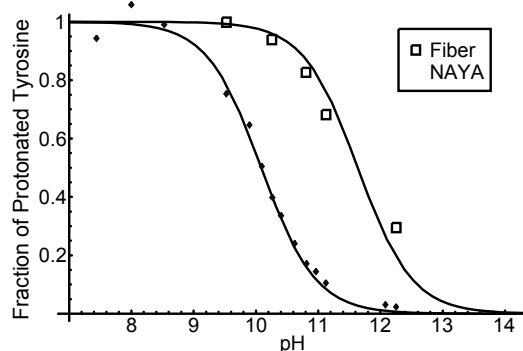

Figure 5. Titration of Y37 in hIAPP$_{fib}$. Titration of 5 mM of hIAPP$_{fib}$ is observed by quenching of Y37 fluorescence intensity. Lower baseline for both NAYA and hIAPP$_{fib}$ correspond to zero intensity. hIAPP$_{fib}$ did not dissolve at high pH, as measured by ThT. 5 mM samples of NAYA show 50 % titration at pH 9.9, consistent with literature values. Curves are plots of the Henderson-Hasselbach equation for a single ionizing species, using pK_as of 9.9 and 11.8, respectively.

DOCKET ALARM

Explore Litigation Insights

Docket Alarm provides insights to develop a more informed litigation strategy and the peace of mind of knowing you're on top of things.

Real-Time Litigation Alerts

Keep your litigation team up-to-date with **real-time alerts** and advanced team management tools built for the enterprise, all while greatly reducing PACER spend.

Our comprehensive service means we can handle Federal, State, and Administrative courts across the country.

Advanced Docket Research

With over 230 million records, Docket Alarm's cloud-native docket research platform finds what other services can't. Coverage includes Federal, State, plus PTAB, TTAB, ITC and NLRB decisions, all in one place.

Identify arguments that have been successful in the past with full text, pinpoint searching. Link to case law cited within any court document via Fastcase.

Analytics At Your Fingertips

Learn what happened the last time a particular judge, opposing counsel or company faced cases similar to yours.

Advanced out-of-the-box PTAB and TTAB analytics are always at your fingertips.

API

Docket Alarm offers a powerful API (application programming interface) to developers that want to integrate case filings into their apps.

LAW FIRMS
Build custom dashboards for your attorneys and clients with live data direct from the court.

Automate many repetitive legal tasks like conflict checks, document management, and marketing.

FINANCIAL INSTITUTIONS
Litigation and bankruptcy checks for companies and debtors.

E-DISCOVERY AND LEGAL VENDORS
Sync your system to PACER to automate legal marketing.

fastcase®
Smarter legal research.